Copolymerization of Norbornene with Ethylene: a High-resolution Liquid NMR, DSC and Solid State NMR Study

Wu-Jang Huang[1], Feng-Chih Chang[1,*] and Peter Po-Jen Chu[2]

1. *National Chiao-Tung University, Institute of Applied Chemistry, Hsin-Chu, 30050 Taiwan, ROC*
2. *National Central University, Dept. of Chemistry Chung-Li, Taiwan, ROC*

Received January 5, 2000; revised February 16, 2000; accepted March 4,2000

Abstract: In this paper, we report the monomer reactivity on the copolymerization of norbornene and ethylene. The reactivity ratios for ethylene (M_1) and norbornene (M_2) are 18.5 and 0.035, respectively. Different copolymerization conditions can produce COC with different microstructures. A ^{13}C NMR shift assignment in pentad sequences in copolymers has been obtained. More isolated polynorbornene or a micro-block length can be obtained using a low Zr/Al catalyst/co-catalyst ratio and at a lower NB/ethylene feed ratio. The T_{1p}^C decay curve shows two component decays in all resonance peaks. These two component decays come from different norbornene microstructures, while the block and alternative have similar T_{1p}^C values.

Keywords: Cyclo olefin copolymer (COC), Monomer reactivity ratio, Solid state NMR, Spin-lattice relaxation time (T_{1p}^C).

Introduction

The copolymerization of norbornene with ethylene leading to cyclo olefin copolymer (COC) and its characterizations has been reported in the literature recently [1-9]. These COC products possess high T_g, high transparency, and a high refraction index, and they have potential applications for electroptical and optical devices [4]. Polymer microstructure has great influence on the properties of the product, which are closely tied to the kinetics of the copolymerization reaction governed by the monomer, catalyst, and reaction conditions. The monomer reactivity ratio (r_1 and r_2) provides direct information on the competition between commoners with a given catalyst.

Previous studies on the reactivity ratio in a COC system by a metallocene catalyst indicated that the cyclo olefin has a low reactivity ratio and an alternative microstructure [9-17]. The reactivity ratio of a copolymer is crucial to understanding the copolymer microstructure and its relationship to the final properties. For example, a block copolymer usually has a relatively higher decomposing temperature (T_d) than a random copolymer or a statistical random copolymer with comparable molecular weight.

A living polymerization system has active centers with long half time. When an active center fails to react with the monomer, it still has the chance to react with a monomer added later. The feed sequence can affect the microstructure of the copolymer and the result is either a more block-like or a more random-like structure.

Knowledge of the copolymer chain sequence reveals important information regarding the chain growth mechanism and kinetics during copolymerization. An unambiguous structure quantification of the COC by the solution NMR has not yet been achieved due to its structural complexity. Furthermore, epimerization of NB may give rise to endo or exo structures in addition to erythro (E) and threo (Z) structures and may cause additional complication in the interpretation of the NMR spectra. Fortunately the strong internal strain in NB bonding makes larger chemical shift differences in the pentad sequence that allow for a clearer detection of the pentad sequence. These results are then compared with the conventional characterization method using block, alternate, and isolate NB segments. The effect of catalyst structure on the reactivity ratio

*To whom all correspondence should be addressed.
Tel: 03-5712121 ext. 56502; Fax: 03-5723764
E-mail: changfc@cc.nctu.edu.tw

J. Polym. Res. is covered in ISI (CD, D, MS, Q, RC, S), CA, EI, and Polymer Contents.

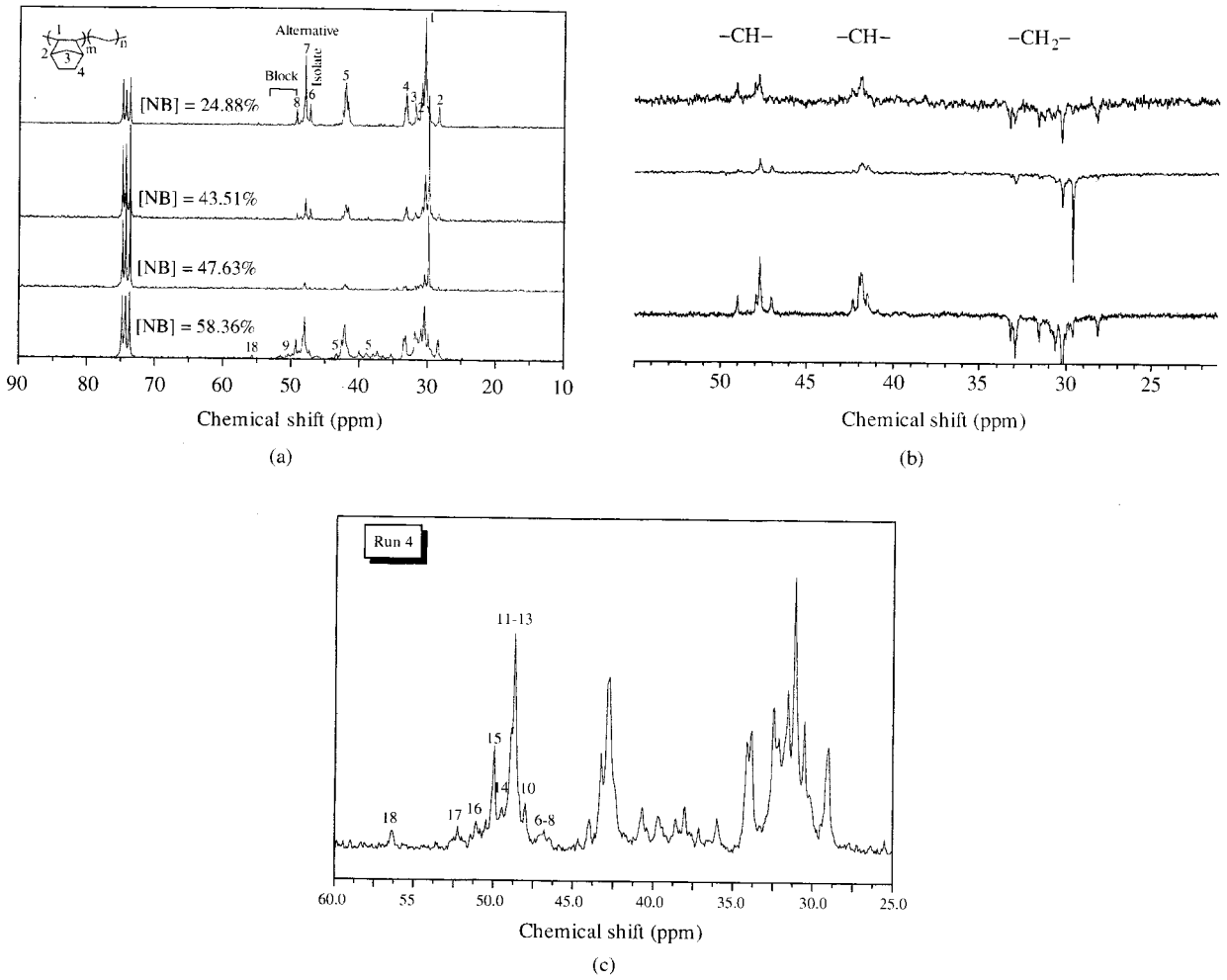

Figure 1. (a) The norbornene-ethylene microstructures and the corresponding liquid state ^{13}C NMR spectra. High resolution and high temperature (333K) ^{13}C NMR spectra of PNB-*co*-PE with variable norbornene content ([NB], mol%). Chemical shift located at 73~76 ppm is the ^{13}C signal from our $C_2D_2Cl_4$ solvent. At the lowest [NB] content, the peak labeled on the spectrum corresponds to the microstructure listed in Table III. At most high [NB] contents, the complex pattern indicates an increase in the amount of norbornene micro-block. The poor resolution and weaker peak of norbornene on the third trace is due to poor solubility in $C_2D_2Cl_4$ solvent. Peaks number 9 and 10 are assigned to the conformation isomer of the NB block and the chain end unit for the first time; in the past these two peaks were unclear. (b) The DEPT-135 experiment results of some samples. The first trace is Run 3, the secondary trace is sample 6, and the lowest trace is Run 5. DEPT experiment results of PNB-*co*-PE are clearly observed in the upper field region; the CH_2 signal is inverted and more down field of the bridge head, while the polymer main chain CH signal is normally maintained in the upper region. (c) Expanded temple of the highest [NB] content (Run 3) spectrum, a more detailed peak assignment was done and the peak labeled focuses on the main chain CH region to clear its chemical shift of different microstructures.

has been determined by comparing our results with results of prior investigations under similar copolymerization conditions.

Experimental

1. General polymerization procedure

COC was polymerized from norbornene and ethylene using an ansa-metallocene catalyst Et (Indenyl)$_2$ZrCl_2 (from Alderich Chemical Co., USA) and MAO co-catalyst(10 wt% in toluene, from Albemaue Chemical Co., USA) [1-4]. The polymerization temperature was controlled at 66 °C using a catalyst/co-catalyst ratio from 3000 to 7000 and the ethylene pressure was maintained at 19~21 psi. Total volume of the system was 60~65 mL during the 2 hrs of polymerization time. The amount of metallocene catalyst was kept at ca. 2 mg. 10-mL acidic methanol was used to terminate the polymerization. The polymer was precipitated by adding an excessive amount of acetone non-solvent and then dried for 8 hrs at 50 °C in a vacuum.

2. Characterization of polymers

^{13}C and DEPT (135°) experimentals on poly-

Table I. ^{13}C NMR chemical shift assignment of pentads in PNB-*co*-PE copolymers.

Band #	Sequence	Microstructure	Chemical shift (ppm)
1	Ethylene block	EEEEE	29.9-30.0 [a]
2	Bridge head	EENNE	28.3 & 31.8
3	2C Bridge	ENENE	32-32.7 [a]
4	1C Bridge	ENENE	33.0-33.7 [a]
5	Bridge head	EENEE	~34.1
6	Bridge head	ENENE	41.5-43 [a]
7	Bridge head	ENNNE	43-44.5
8	Isolate NB	EENEE	46.74
9		EENEN	46.78, 46.9
10	Alternate NB	NENEN	47.43
11		EENNE	47.48, 47.65
12		NENNE	48.13, 48.16
13		NNENN	48.18-48.29 [b]
14		EENNN	48.72, 48.77
15		ENNNE	48.94
16		NENNN	49.45-49.69
17		NENNN	50.8-52 [b]
18	(Chain end)	C-OCH_3	56.2 [b]

(a) Means the popularly accepted assignment peak [9,13,17].
(b) From this work.

mers were characterized by a Bruker 200 MHz high resolution NMR using trichlorobenzene (TCB) as the solvent and $CDCl_3$ as the lock solvent at room temperature. Since the products from Run 1 and Run 4 could not be completely dissolved in the solvent for resolved ^{13}C NMR characterization, ^{1}H NMR was used instead to give approximated structure characteristics from the broad NMR resonance [14]. Thermal transition temperatures were determined by a Perkin-Elmer DSC-7 with heating and cooling rates of 10 °C/min and scanning ranges from 30 to 220 °C or 300 °C. Norbornene microstructures were determined from the peak integrated values of the region of 42~49 ppm chemical shift. Activity of polymerization was calculated from polymer weight, catalyst amount and polymerization time.

Results and Discussion

1. Polymer microstructure characterized by high resolution NMR

The microstructures of the polynorbornene-co-ethylene copolymers and their corresponding high temperature liquid state ^{13}C NMR and DEPT (135°) spectra are shown in Figures 1(a), 1(b) and 1(c). Peak assignments for the NB-*co*-PE chemical shift of various structural segments are tabulated in Table I and the corresponding pentad segments are assigned wherever possible. Many earlier papers have reported the peak assignments on PNB-*co*-PE copolymers, but most of them have focused on co-

Table II. Microstructure distribution of NB in PNB-*co*-PE[a] by solution ^{13}C NMR.

Sample	NB feed (g/L)	NB content (mol %)	NB Micro (%)		
			Block	Alternative	Isolate
1	308.0	100.0	100	0	0
2	558.0	ND	ND	ND	ND
3	558.0	58.36	40.16	51.85	7.99
4	249.4	47.63[b]	>50[b]	–	–
5	175.9	43.51	17.33	66.60	16.07
6	78.52	24.88	21.02	51.04	27.98

(a) Polymerization condition: Ethylene pressure = 20 psi, 70 °C; total volume = 60 mL ; [Al]/[Zr] = 8000~4000 ; catalyst = 1~2 mg.
(b) Estimated from ^{1}H NMR (see text).

Table III. Activity and thermal properties of metallocene catalyzed poly (norbornene-*co*-ethylene)[a].

Sample	NB feed (g/L)	[Al]/[Zr]	Activity (Kg/mol · hr)	T_g[b] (°C)	T_m (°C)
1	308.0	7815	325.0	136.2	–
2	574.6	662	37.20	ND	–
3	558.0	7775	408.8	102.5	–
4	249.4	7775	708.7	81.3	–
5	176.9	3947	1000	86.8	–
6	78.52	3947	1200	68.1	129.67
7	0.0	7815	2500	< 0	122.45

(a) Co-catalyst: MAO, total volume of toluene solution is about 60 mL.
(b) Sample as prepared.

polymers with low norbornene content except for a few cases [9,17]. The norbornene microstructure could be obtained from the norbornene C-H resonance region (48.9~49.9 ppm) that corresponds to isolate, block and alternative microstructures [13-16]. Previous 2D NMR on low molecular weight polynorbornene-*co*-polypropylene copolymers indicated that the complex NMR pattern derives mainly from the norbornene dimmers, trimmers and their induced gamma-gauche effect [18,19]. Table II summarizes the calculated norbornene content and the corresponding microstructure of the copolymer based upon ^{13}C NMR [11-16].

2. Polymerization activity and DSC analysis

The polymerization conditions, reactivities and the thermal properties of the corresponding COC copolymers are summarized in Table III. Run 7 represents the pure polyethylene activity (2.5×10^{6}~10^{5} g/mole hr), which is typical for this metallocene catalyst. In comparison, Run 1 (PNB homopolymer) shows about one order lower of the activity with the same catalyst under the same polymerization

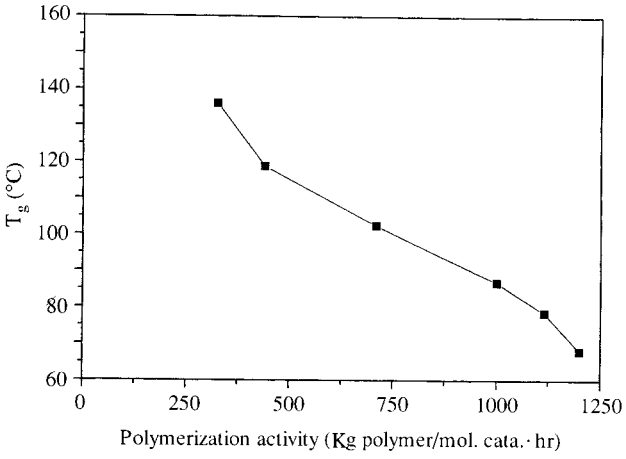

Figure 2. The almost linear reduction of T_g with increasing activity.

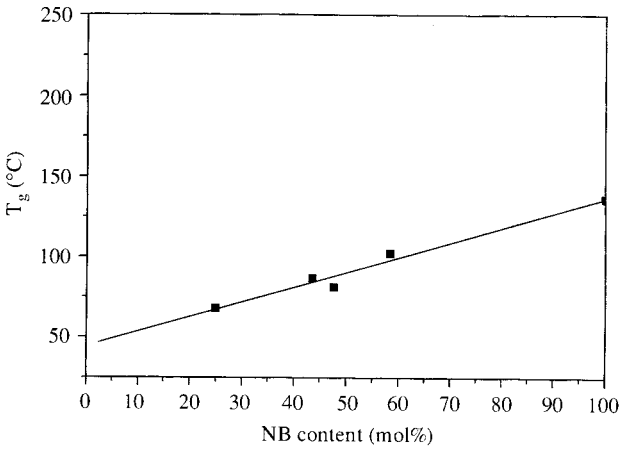

Figure 3. Relationship between [NB] content and T_g of the sample as prepared.

conditions. Run 2 and Run 3 compare the effect of the catalyst/co-catalyst ratio using the same norbornene/ethylene feed concentration; the results show about a twenty-fold increase in the activity when the Al/Zr ratio is increased from 662 to 7775.

Runs 3~6 compare the effect of NB feed concentration with identical Al/Zr ratios at 7775 (Runs 3, 4) and 3947 (Runs 5, 6), respectively. In both cases, a higher norbornene feed concentration leads to a decrease in the polymerization activity. When the PE content is greater than 50 mol%, both the PE crystalline melting temperature (T_m) and the PNB glass transition temperature (T_g) can be observed from the DSC analyses. Figure 2 shows that the T_g decreases with increasing polymerization activity (i.e., an increase in the NB content of the copolymer). In view of the relatively higher PE activity, this correlation merely reflects the larger difference in the reactivity ratio of NB and ethylene monomers during copolymerization. In general, an increase in the norbornene feed ratio leads to an increase in the norbornene content of COC [1,3].

Figure 3 shows the plot of T_g versus the NB content in the COC copolymers. The T_g of the sample as prepared increases linearly with the NB content, an indication of a gradual stiffening of the COC chain with increasing NB content.

In the NB rich samples, NB block structure dominates. In the relatively lower NB content copolymers, alternating and isolated NB microstructures are favorable (Table II). In the latter case, a long continuous PE block is observed, which gives rise to crystallization behavior in thermal analysis. Due to the significant difference in monomer reactivity between ethylene and norbornene (about 500 fold), it is difficult to achieve block NB unless the NB feed content far exceeds that of the PE. In most cases, NB appears only in the alternate and isolated microstructures [5,9,10].

3. Monomer reactivity ratio

The catalyst structure is important in controlling the reactivity ratio. Although a definite conclusion cannot be drawn without the detailed molecular modeling of the reaction intermediately involving both monomers general qualitative trends can be observed nevertheless. In this study, we report the r_1 and r_2 value for PNB-*co*-PE copolymerization at 66.8 °C (~70 °C) in toluene, which is the most common polymerization condition that has been employed. The monomer reactivity ratios of COC copolymerization under this condition have never been reported as far as we know. Figure 4 shows the plot of F_1 versus f_1. According to the Fineman-Ross equation, r_1 and r_2 are defined as the reactivity ratio of monomer 1 (ethylene) and monomer 2 (norbornene). The solid line represents the PNB-*co*-PE system and the dotted lines represent different (r_1, r_2) cases. Table IV lists the reactivity ratios for ethylene and norbornene with various catalysts from the literature and from this work for comparison [6,9,10,13,16,17]. When the temperature is increased the $r_1 \times r_2$ product becomes larger in the polynorbornene-*co*-polyethylene case using $Et(Indenyl)_2ZrCl_2$/MAO catalysts.

4. Solid state relaxation time study

Due to the main chain rigidity of the COC, the segment motion at room temperature is limited and results in high $T_{1\rho}^H$ values. For all PNB-*co*-PE copolymers, their $T_{1\rho}^H$ values are not affected by the NB content [20]. Solid state NMR (SS-NMR) ^{13}C spin-lattice relaxation time on rotating frame ($T_{1\rho}^C$) decay curve shows two component decays for all ^{13}C peaks (shown in Figure 5). The fraction of fast and slow decay $T_{1\rho}^C$ components resulted from

Table IV. Monomer reactivity ratio of metallocene catalyzed norbornene base copolymers.

Catalyst	Source	T_p (°C)[a]	r_1[b]	r_2[b]	$r_1 \times r_2$
$(Cp)_2ZrCl_2$	Ref [17]	40	4.0	0.03	0.12
$[MeCH(Cp)_2]ZrCl_2$	Ref [17]	70	0.83	0.29	0.241
$Et(Ind)_2ZrCl_2$	Ref. [2]	25	6.6	0.030	0.198
$Et(Ind)_2ZrCl_2$	Ref. [17]	40	1.9	0.030	0.057
$Et(Ind)_2ZrCl_2$	This work	70	18.5	0.035	0.629
$Me_2Si(Ind)_2ZrCl_2$	Ref. [17]	30	2.66	0.36	0.958
$Et(Ind\ H_4)_2ZrCl_2$	Ref. [17]	25	2.2	0.037	0.081
$Et(Ind\ H_4)_2ZrCl_2$	Ref. [17]	70	6.8	0.044	0.299
*i*Pr[IndCp]$ZrCl_2$	Ref. [17]	70	0.88	0.05	0.044
*i*Pr[(3-MeCp)Ind]$ZrCl_2$	Ref. [17]	70	1.14	0.100	0.114
*i*Pr[(3-BuCp)Ind]$Zrcl_2$	Ref. [17]	70	1.1	0.026	0.029
$Ph_2C[(Flu)(Cp)]ZrCl_2$	Ref. [17]	0	2.0	0.05	0.100
$Ph_2C[(Flu)(Cp)]ZrCl_2$	Ref. [17]	30	3.0	0.05	0.150
$Me_2C[(Flu)(Cp)]ZrCl_2$	Ref. [17]	30	3.4	0.06	0.204
$Me_2C[(Flu)(Cp)]ZrCl_2$	Ref [17]	40	1.8	~0	0
$Me_2C[(Flu)(Cp)]ZrCl_2$	Ref [17]	70	1.3	0.03	0.039
$Me_2C[(Flu)(3\text{-}i\text{PrCp})]ZrCl_2$	Ref [17]	30	4.15	0.033	0.137
$Me_2C[(Flu)(t\text{-BuCp})]ZrCl_2$	Ref. [17]	30	3.1	0	0

(a) Polymerization temperature.
(b) r_1: ethylene monomer reactivity ratio, r_2: norbornene monomer reactivity ratio.

Table V. Comparison of norbornene microstructure with SS-NMR T_{1p}^C.

Run	Norbornene Microstructure[a]		SS-NMR[b]	T_{1p}^C
	Isolate (%)	Block + Alternative (%)	Fast decay (%)	Slow decay (%)
1	0	100	–	–
3	7.99	92.01	10.09	90.91
5	16.07	83.93	14.71	85.31
6	27.98	72.02	31.00	69.00

(a) Obtained from high resolution NMR.
(b) Obtained from solid state NMR.

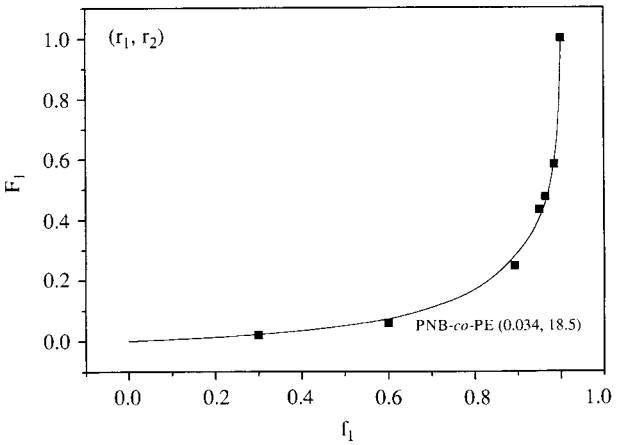

Figure 4. Plot of F_1 *vs.* f_1; the Fineman-Ross equation is used to fit the experimental data (r_1,r_2)= reactivity of monomer 1 (ethylene) and monomer 2 (norbornene), respectively. The solid line represents the PNB-*co*-PE system. The dotted line represents the different (r_1, r_2) cases.

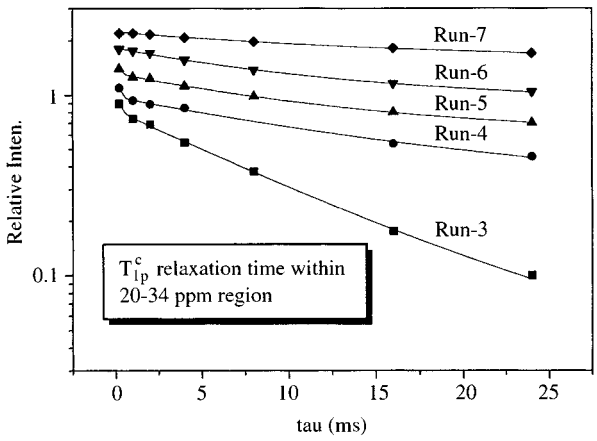

Figure 5. Decay curves of the CH_2 peak in poly(norbornene-ethylene) copolymers.

the norbornene C-H peak being consistent with the previously determined norbornene microstructure contents (shown in Table V). This reflects the fact that these two components resulted from different norbornene microstructures, block and alternative microstructures, having similar T_{1p}^C values.

Conclusions

We report on the monomer reactivity of the polymerization of norbornene and ethylene. Different copolymerization conditions can produce COC with different microstructures. Isolated polynorbornene or a micro-block length can be obtained

with a low Zr/Al ratio at a lower NB/ethylene feed ratio. The T_{1p}^{C} decay curve shows two component decays at all resonance peaks, resulting from different norbornene microstructures. The block and alternative microstructures have similar T_{1p}^{C} values.

Acknowledgment

Financial support of this research was provided by the National Science Council of the Republic of China under contract number NSC-88-2113-M-008-004.

References

1. A. Kaminsky, A. Bark and M. Arndt, *Macromol. Chem., Macromol. Symp.*, **47**, 83 (1991).
2. W. Kaminsky, M. Arndt and A. Bark, *Polym. Preprints*, **32**, 467 (1991).
3. W. Kaminsky and A. Bark, *Polym. Int.*, **28**, 251 (1992).
4. G. M. Benedikt, B. L. Goodall, N. S. Marchant and L. F. Rhodes, *New J. Chem.*, **18**, 105 (1994).
5. N. Herfert, P. Montag and G. Fink, *Makromol. Chem.*, **194**, 3167 (1993).
6. W. Kaminsky, *Macromol. Chem. Phys.*, **197**, 3907 (1996).
7. G. Guerra, V. M. Vitaliano, C. D. Rosa, V. Petraccone and P. Corradini, *Macromolecules*, **23**, 1539 (1990).
8. W. Kaminsky, R. Engehausen and J. Kopf, *Angew. Chem. Int. Ed. Engl.*, **34**, 2273 (1995).
9. D. Ruchatz and G. Fink, *Macromolecules*, **31**, 4681 (1998).
10. D. Ruchatz and G. Fink, *Macromolecules*, **31**, 4674 (1998).
11. H. Cherdron, M.-J. Brekner and F. Osan, *Angew. Makromol. Chem.*, **223**, 121 (1994).
12. C. H. Bergstrom, T. L. J. Vaananen and J. V. Seppala, *J. Appl. Polym. Sci.*, **63**, 1071 (1997).
13. C. H. Bergstrom, T. L. J. Vaananen and J. V. Seppala, *J. Appl. Polym. Sci.*, **67**, 385 (1998).
14. C. H. Bergstrom, T. L. J. Vaananen and J. V. Seppala, *J. Polym. Sci., Polym. Chem.*, **36**, 1633 (1998).
15. C. H. Bergstrom and J. V. Seppala, *J. Appl. Polym. Sci.*, **63**, 1063 (1997).
16. T. Rische, A. J. Waddon, L. C. Dickinson and W. J. Macknight., *Macromolecules*, **31**, 1871 (1998).
17. A. L. Mcknight and R. M. Waymouth, *Macromolecules*, **32**, 2816 (1999).
18. P. P. Chu and M. S. Teng, *J. Polym. Sci., Polym. Chem.*, (submitted).
19. T. F. A. Haselwander, W. Heitz, S. A. Krugel and J. H. Wendroff, *Macromol. Chem. Phys.*, **197**, 3435 (1996) .
20. P. P. Chu, W. J. Huang and F. C. Chang, unpublished data.